

Highlights:

Direct coal liquefaction residue was firstly extracted at 25 °C by liquefied DME;

It achieved a higher yield than those by Soxhlet method using acetone or hexane;

The extract had a high content of C and low contents of S, O, and ash (< 0.1%);

Abundant polycyclic aromatic hydrocarbons in the extract were determined;

DME extraction is as good as acetone Soxhlet extraction on molecular compositions.

1
2
3
4
5
6
7
8
9
10
11
12
13
14
15
16
17
18
19
20
21

Room-Temperature Extraction of Direct Coal Liquefaction Residue by Liquefied Dimethyl Ether

Qingxin Zheng, ^{a*} Yelin Zhang, ^a Wahyudiono, ^a Thierry Fouquet, ^b Xi Zeng, ^c Hideki Kanda, ^{a*}
Motonobu Goto ^a

^a Department of Materials Process Engineering, Graduate School of Engineering, Nagoya University,
Furo-cho, Chikusa, Nagoya 464-8603, Japan.

^b Polymer Chemistry Group, Research Institute for Sustainable Chemistry (ISC), National Institute of
Advanced Industrial Science and Technology (AIST), Central 5, 1-1-1 Higashi, Tsukuba, Ibaraki 305-
8565, Japan.

^c State Key Laboratory of Multi-Phase Complex Systems, Institute of Process Engineering, Chinese
Academy of Sciences, Beijing 100190, China.

* Corresponding author.

E-mail addresses: zhengqx1984@gmail.com (Q. X. Zheng) and
kanda.hideki@material.nagoya-u.ac.jp (H. Kanda).

22 **Abstract**

23 Direct coal liquefaction residue (DCLR) is the main byproduct during the direct coal liquefaction
24 process. The efficient recovery of organic components from DCLR at low temperatures is beneficial for
25 improving the economy and reducing energy consumption and environmental pollution. Here, DCLR
26 was extracted using liquefied dimethyl ether (DME), acetone, and hexane as the solvents. Compared
27 with the other two solvent Soxhlet extraction, the DME extraction process was performed at room
28 temperature with the shortest extraction time, the lowest energy consumption, and the highest extraction
29 yield (16.2%). Owing to the high carbon contents, low sulfur and oxygen contents, and low ash contents
30 (< 0.1%), the extracts obtained using liquefied DME and acetone naturally became the feedstock of
31 carbon materials. Based on the results of the gas chromatography-mass spectrometry analysis, the
32 extracts obtained using the three different solvents had similar compositions in light compounds and
33 were abundant in polycyclic aromatic hydrocarbons with two-, three-, four-, five-, and six-membered
34 benzene rings, indicating that all three DCLR extracts are potential raw materials for preparing high
35 value-added carbon materials. Furthermore, the molecular composition analysis revealed that the room-
36 temperature extraction using liquefied DME was as good as high-temperature Soxhlet extraction using
37 acetone, considering the similarity of their compositions in high molecular weight species and the
38 considerably higher efficiency than that of high-temperature Soxhlet extraction using hexane. Due to the
39 low energy consumption, short extraction time, high extraction yield, and high performance of the
40 extract, liquefied DME is an efficient and economic solvent for extracting DCLR.

41

42 **Keywords:** Direct coal liquefaction residue; extraction; room temperature; liquefied dimethyl ether;
43 polycyclic aromatic hydrocarbons; molecular composition.

44

45 **1. Introduction**

46 The processes of direct coal liquefaction (DCL) and indirect coal liquefaction (ICL) are the two most
47 important technologies used to convert coal into liquid fuels and chemicals [1]. In the DCL process, vast
48 quantities (~0.5 million t/a) of an undesirable byproduct commonly called the DCL residue (Hereafter,
49 referred to as DCLR), accounts for 20-30 wt% of the raw coal consumed in the DCL process and has
50 emerged as a serious problem for industrial application [2, 3]. DCLR contains high-boiling-point
51 liquefied oils, asphaltenes, unreacted coal, mineral matter, and liquefaction catalysts [4]. In light of the
52 economic and environmental considerations, DCLR must be effectively utilized.

53 DCLR was primarily used as a feedstock for combustion, gasification, pyrolysis, and carbonization to
54 produce heat, fuel gas, tar, and coke, respectively [5-8], which have low market values and may cause
55 additional environmental problems. The organic components in DCLR, such as liquefied oil and
56 asphaltenes, are valuable products. In particular, because of the abundance of polycyclic aromatic
57 structures (PASs) [9], DCLR is considered an excellent precursor for preparing various high-grade
58 carbon materials, such as carbon micro/nanofibers [10, 11] and porous carbons [12, 13].

59 The solvents, which have been used for extracting DCLR, can be classified into three groups: traditional
60 organic solvents, water, and ionic liquids. Up to now, DCLR has been extracted by using various
61 traditional organic solvents, such as acetone [2], methanol [14], ethanol [14], isopropanol [2, 14],
62 dipropylamine [9, 15], toluene [16], and benzene [2, 16, 17]; the energy cost is moderate, but most of the
63 solvents used are toxic. Subcritical water extraction, using hot water (100-374 °C) as the only solvent, is
64 a green and efficient method to extract organic components from DCLR [18]; however, the high energy
65 consumption due to high extraction temperature and requirements of apparatus resistant to high
66 temperature and pressure may greatly limit its industrial application. By comparison, ionic liquids are
67 more suitable for extracting DCLR, because the extraction is conducted at room temperature and most
68 ionic liquids are green solvents [3, 19-24]. However, ionic liquids are much more expensive than other
69 organic solvents, and the process of separating the extract from the solvent is highly complex [18].

70 **Table 1** The ultimate and proximate analyses of DCLR sample, and extracts and residues after
 71 extraction processes.

| Sample name | Ultimate analysis [wt%, daf] ^a | | | | | Atomic ratio [-] | | Proximate analysis [wt%, db] ^b | | | Moisture [wt%] |
|-------------|--|-----|-----|-----|-----------|---------------------|------|--|------|------|-------------------|
| | C | H | N | S | O (diff.) | H/C | O/C | FC | VM | Ash | |
| DCLR | 77.1 | 3.9 | 1.0 | 1.9 | 16.1 | 0.60 | 0.16 | 42.4 | 42.6 | 15.0 | 0.64 |
| DME-R | 75.6 | 3.8 | 0.9 | 2.1 | 17.6 | 0.59 | 0.17 | 47.4 | 36.9 | 15.7 | -- |
| DME-E | 88.9 | 6.8 | 1.2 | 0.3 | 2.8 | 0.92 | 0.02 | 7.8 | 92.1 | 0.1 | -- |
| Acetone-R | 75.3 | 3.7 | 0.9 | 2.0 | 18.1 | 0.59 | 0.18 | 49.9 | 34.4 | 15.7 | -- |
| Acetone-E | 88.9 | 6.4 | 1.3 | 0.2 | 3.2 | 0.86 | 0.03 | 5.2 | 94.7 | 0.1 | -- |
| Hexane-R | 77.0 | 3.9 | 1.0 | 1.9 | 16.2 | 0.60 | 0.16 | 46.7 | 38.8 | 14.5 | -- |
| Hexane-E | 82.6 | 6.7 | 0.6 | 0.1 | 10.0 | 0.97 | 0.09 | 2.5 | 96.0 | 1.5 | -- |

72 ^a daf means dry ash-free basis; ^b db means dry basis.

73
 74 Therefore, a non-toxic, economical, and effective solvent is particularly desired for extracting organic
 75 components from DCLR.

76 Dimethyl ether (DME, CH₃OCH₃), which is the simplest ether, is a colorless gas with a slight ether-like
 77 fragrance at ambient temperature and pressure. The boiling point, critical temperature, and critical
 78 pressure of DME are -24.2 °C, 128 °C, and 5.4 MPa, respectively. At normal ambient temperature, DME
 79 is easily compressed, and liquefied DME dissolves 7-8% by the weight of water [25]. DME is non-
 80 reactive, non-toxic, non-carcinogenic, and does not induce pH change in aqueous solution [26].
 81 Furthermore, it has a competitively low price and is a safe solvent for use in the field of food processing
 82 [27]. Thus, it can be adequately safe and economic to adapt DME in an extraction process.

83 Compared to other techniques, extraction using liquefied DME has the advantages of non-toxicity, low
 84 operating temperature (room temperature), short extraction time, simple operational process, and
 85 environmental compatibility. Liquefied DME can extract water, lipids, or functional ingredients from
 86 various feedstocks [28]. All the DME extraction processes are performed at low temperatures (including
 87 room temperature) in the range from 20 to 60 °C and under pressures ranging from 0.5 to 1.4 MPa.
 88 Herein, ‘room temperature’ is defined by the Japanese Pharmacopeia as 1-30 °C [29]. Furthermore, due
 89 to the low boiling point, liquefied DME can evaporate at room temperature after the extraction process
 90 without heating, which is beneficial for reducing energy consumption and improving the economy of the

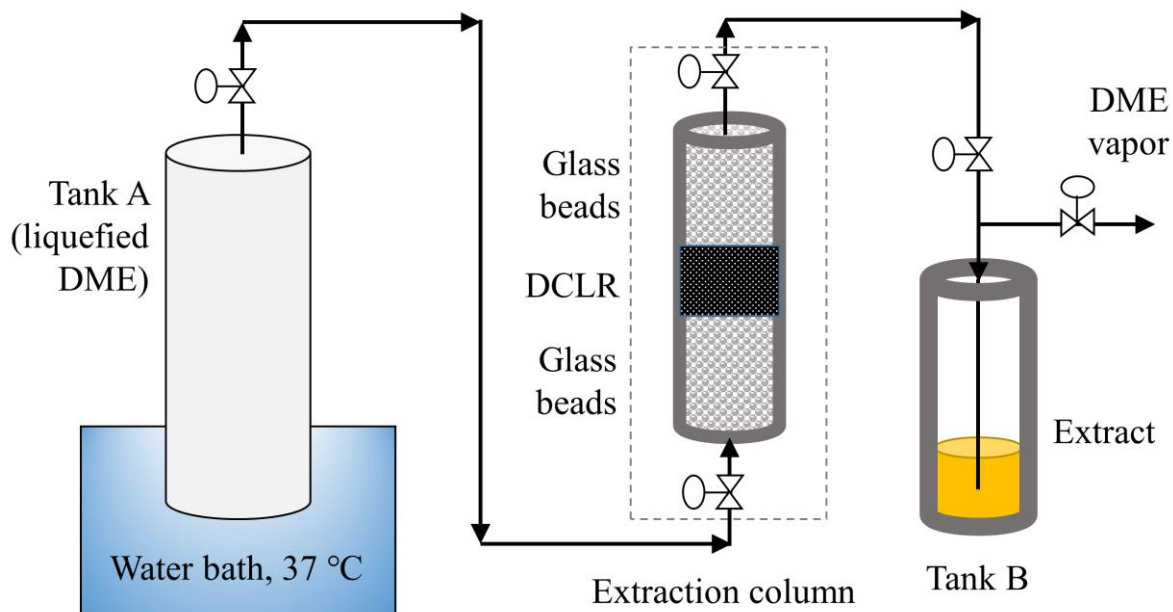


Figure 1 Schematic diagram of the DME extraction apparatus.

DCL process.

Here, we conducted the room-temperature extraction of DCLR using liquefied DME as the solvent, compared it with those by the traditional Soxhlet method using acetone and *n*-hexane as the solvents, and studied the yield, elemental composition, compound composition, and molecular composition of the extracts in detail.

2. Material and Methods

2.1. Materials and solvents

The raw DCLR sample was obtained from Shenhua direct coal liquefaction plant in China. **Table 1** shows the ultimate and proximate analysis results of the DCLR sample. The DCLR sample has a low moisture content of 0.64 wt%, a high ash content of 15.0 wt%, and 77.1 wt% of C and 3.9 wt% of H (H/C = 0.60). The contents of volatile matter (VM) and fixed carbon (FC) are close, at 42.4% and 42.6%, respectively. Before the extraction process, the DCLR sample was grounded and sieved by a 250 μm sieve.

106 The solvents for extraction included acetone (for high performance liquid chromatography (HPLC);
107 FUJIFILM Wako Pure Chemical Corp., Osaka, Japan), *n*-hexane (for HPLC; FUJIFILM Wako Pure
108 Chemical Corp., Osaka, Japan), and liquefied DME (Spray-work aircan 420D; Tamiya Inc., Shizuoka,
109 Japan).

110 **2.2. DME extraction process**

111 **Figure 1** schematically shows the laboratory-scale DME extraction apparatus. A tank containing
112 liquefied DME (tank A; volume: 1000 cm³; Taiatsu Techno Corp., Saitama, Japan), an extraction
113 column (diameter: 11.6 mm, length: 190 mm; HPG-10-5; Taiatsu Techno Corp., Saitama, Japan), and a
114 collection tank (tank B; HPG-96-3; Taiatsu Techno Corp., Saitama, Japan) were connected in series. In a
115 typical experiment, 3 g of DCLR sample was used as the raw material. After the DCLR sample was
116 loaded into the extraction column, glass beads (diameter between 1.5 and 2.5 mm; BZ-2, AS ONE Corp.,
117 Osaka, Japan) were loaded at the top and bottom ends of the column. The liquefied DME in tank A was
118 maintained at 37 ± 1 °C in a water bath, and its saturated vapor pressure was 0.82 ± 0.02 MPa. The
119 liquefied DME was supplied from tank A and flowed to the extraction column owing to the pressure
120 difference between tank A and the extraction column. The DME flow rate was maintained at ~8 mL/min
121 by controlling a valve at the outlet of the extraction column. Through a long tube between tank A and
122 the extraction column, DME was cooled down, and the extraction was performed at 25 °C in the
123 extraction column. After the liquefied DME passed through the extraction column at different time
124 intervals, DME was evaporated by opening the pressure-reducing valve of tank B. The total extraction
125 time was less than 60 min. After the extraction, the residue and extract (referred to as ‘DME-R’ and
126 ‘DME-E’, respectively) were collected from the extraction column and tank B, respectively, and
127 weighed. The consumption of DME during the extraction process was calculated by the mass difference
128 of liquefied DME in tank A.

129 **2.3. Soxhlet extraction process**

130 DCLR was extracted by acetone and hexane (*n*-hexane), respectively, using a Soxhlet apparatus
131 (Vidrolabor®). In each experiment, 3 g of DCLR sample and 200 mL of solvent were used for the
132 extraction. The refluxing started at temperatures above the boiling points of the solvents, which are 56.5 °C
133 and 69 °C for acetone and hexane, respectively. After the extraction proceeded for 6 h, the solvent was
134 separated from the extract at 60 °C under reduced pressure using a rotary evaporator. The residues and
135 extracts were dried, collected, kept in sealed glass vessels, and stored in a refrigerator until further
136 analysis. They are referred to as ‘Acetone-R’, ‘Hexane-R’, ‘Acetone-E’, and ‘Hexane-E’, in which ‘R’
137 and ‘E’ refer to the residue and extract, respectively.

138 **2.4. Characterization**

139 The elemental composition of the solid product was determined using a CHNS analyzer (2400 CHNS/O
140 Series II System; PerkinElmer Inc., MA, USA). The moisture content was tested by using a halogen
141 moisture meter (65g0001g; AS ONE Corp., Osaka, Japan). The VM, FC, and ash contents were
142 measured using a thermogravimetric analyzer (TG 8120; Rigaku Corp., Osaka, Japan). According to the
143 National Institute of Standard and Technology (NIST) mass spectral database, light compounds in the
144 extracts were identified by gas chromatography-mass spectrometry (GC-MS) (7890A GC system and
145 5975C inert XL MSD with a triple-axis detector; Agilent Technologies, Inc., CA, USA) using a
146 diphenyl-dimethylpolysiloxan column (DB-5; 30 m × 0.25 mm × 0.25 μm; Agilent Technology Tokyo
147 Ltd, Japan) and tetrahydrofuran (THF; stabilizer free for HPLC; ≥ 99.8%; Wako Pure Chemical
148 Industries, Ltd., Osaka, Japan) as the solvent. The chromatograph was temperature-programmed from 40
149 to 300 °C at a rate of 5 °C/min. The injection volume of the sample was 1 μL and He was used as the
150 carrier gas with a flow rate of 24 mL/min.

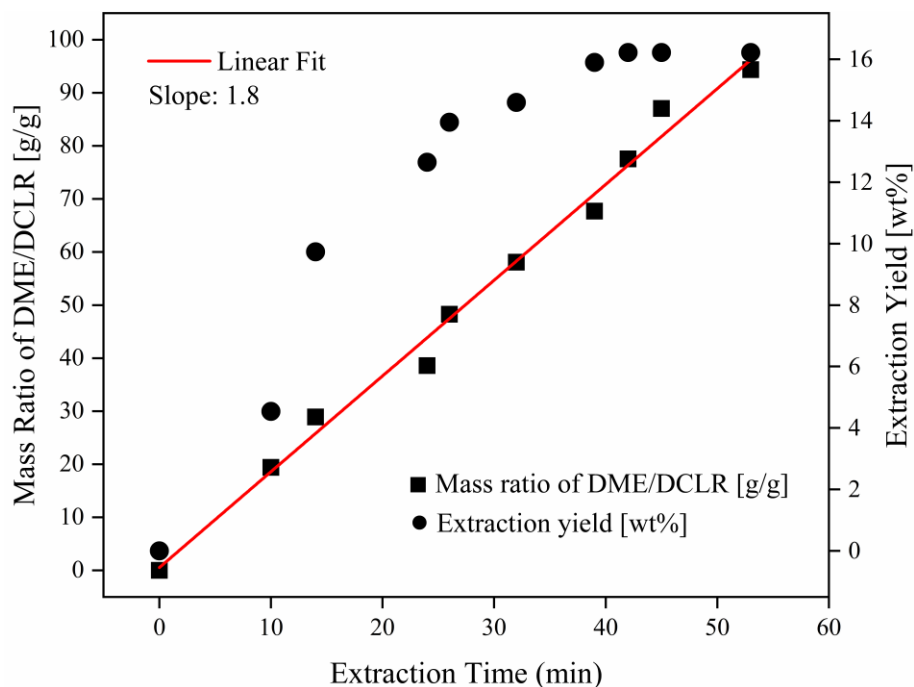
151 The extraction yield was defined as the percentage of the mass of extract against the total mass of the
152 raw DCLR sample excluding moisture and ash. The calculation equation (Eq. 1) is shown as follows.

$$153 \text{ Extraction yield} = \frac{\text{Mass of extract (g)}}{\text{Mass of raw DCLR (g)}} \times 100\% \quad (1)$$

154 **2.5. Mass and Kendrick mass defect analyses**

155 All the chemicals for mass analyses were purchased from Wako Pure Chemicals (Osaka, Japan) unless
156 otherwise mentioned. The laser desorption ionization high-resolution mass spectra (LDI-HRMS) were
157 recorded using a JMS-S3000 spiralTOFTM instrument (JEOL, Tokyo, Japan) operated in positive ion
158 mode. First, 0.5 μ L of the extracts solubilized in THF at 1 mg/mL was deposited on a disposable target
159 plate (Hudson Surface Technology, NJ, USA) to form a thin layer. This was repeated three times for
160 confirming repeatability of the LDI-HRMS fingerprint and three times for internal calibration using the
161 sodium adducts of sodium trifluoroacetate (NaTFA) and [3-(4-tert-butylphenyl)-2-methyl-2-
162 propenylidene]malononitrile for the low mass range of <300 Da and 600 g/mol
163 poly(methylmethacrylate) for the high mass range up to 700 Da. The voltages, delay time, and laser
164 fluence were adjusted once to record a satisfactory signal just above the desorption threshold with
165 resolving at \sim 45000 along the entire mass range and further kept identical for all the extracts for the sake
166 of comparison. Instrument control, data acquisition, and preliminary processing of all the experiments
167 were achieved using MSTornado provided by JEOL.

168 The Kendrick mass defect (KMD) analyses and assignments of the ion series were done from the peak
169 lists generated with mMass 5.5.0 (no deisotoping, threshold at 1% for a rapid comparison of the
170 composition with simple KMD plots) using “Kendo” [30], which is a homemade Excel spreadsheet
171 available upon request with Visual Basic for Application coding (VBA) [31]. The resolution-enhanced
172 KMD plots displaying the mass defects (i.e., the fractional part of the accurate mass of an ion with
173 regard to a chosen reference mass) as a function of the mass-to-charge ratio of the detected ions (noted
174 m/z) were computed using a mathematical base unit, CH_2/X , with the CH_2 methylene chemical moiety at
175 14.01565 Da and X as the natural divisor. The separating power of the resolution-enhanced KMD plot
176 was modified from its regular counterpart and computed with CH_2 only [32] depending on X. The values
177 of X were set at 13 (actual base unit: $\text{CH}_2/13=1.07813$), 20 (actual base unit: $\text{CH}_2/13=0.70078$), and 21
178 (actual base unit: $\text{CH}_2/13=0.66741$) in the KMD plots reported below to separate the carbonaceous ion



179

180 **Figure 2** The relationship among extraction time, DME consumption, and extraction yield. ■ Mass ratio
 181 of DME/DCLR; ● Extraction yield.

182 series by their contents of H, O, and N atoms and ^{13}C isotopes in visual graphs with unambiguous
 183 assignments.

184 3. Results and Discussion

185 3.1. Extraction of DCLR by liquefied DME

186 **Figure 2** shows the relationship between extraction time, DME consumption, and extraction yield. DME
 187 consumption exhibits a linear relationship with extraction time with a slope of 5.4 g/min and is displayed
 188 by black solid cubes and read line (linear fit) in **Figure 2**. The difference between the theoretical and
 189 actual values of the DME consumption can be attributed to the errors caused by the interval procedure.
 190 As shown by black solid circles in **Figure 2**, the extraction yield increases with the liquefied DME flow
 191 during the first 10 min. For an extraction time of 10 to 24 min, the mass ratio of DME/DCLR changed
 192 from 20 to 39, and the growth rate of the extraction yield reached a maximum. Subsequently, the
 193 extraction yield increased slowly and remained unchanged at 16.2%, indicating that the extraction was

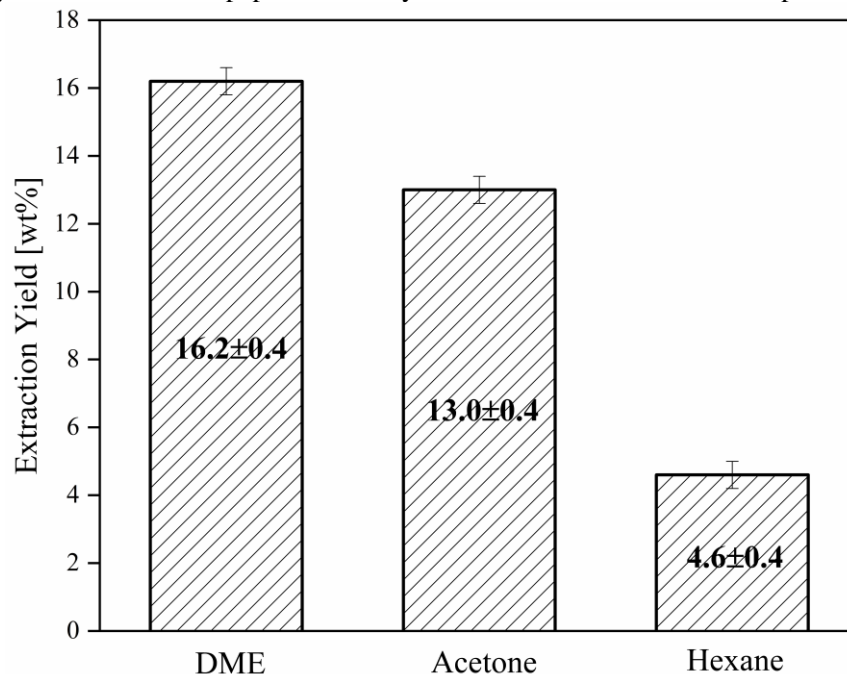
194 **Table 2** Performance comparison of the extraction methods using liquefied DME and subcritical water
 195 as solvents.

| Solvents | Temperature [°C] | Pressure [MPa] | Time [min] | Mass ratio of Solvent/DCLR [g/g] | Yield 1 [wt%] ^a | Yield 2 [wt%] ^b | Yield 3 [wt%] ^c |
|------------|------------------|----------------|------------|----------------------------------|----------------------------|----------------------------|----------------------------|
| DME | 25 | 0.6~0.8 | 40 | 70 | -- | 13.8 | 16.2 |
| | 250 | 5.2 | 120 | 15 | 6 | 3.6 | -- |
| | 320 | 11.7 | 120 | 10 | ~6 | ~3.6 | -- |
| Water [18] | 300 | 8.9 | 60~180 | 15 | 12~14 | 7.2~8.4 | -- |
| | 300 | 8.9~11.6 | 120 | 15 | ~14 | 8.4 | -- |
| | 320 | 11.7 | 120 | 15 | 24 | 14.4 | -- |
| | 320 | 11.7 | 120 | 30 | ~30 | ~18.0 | -- |
| | 320 | 11.7 | 120 | 90 | ~51 | ~30.7 | -- |

196 ^a: Yield reported [18] on the dry basis of THF-extractable fraction in the DCLR sample via Soxhlet
 197 extraction.

198 ^b: Yield recalculated on the dry basis of the DCLR sample.

199 ^c: Extraction yield defined in this paper, on the dry ash-free basis of the DCLR sample.



200

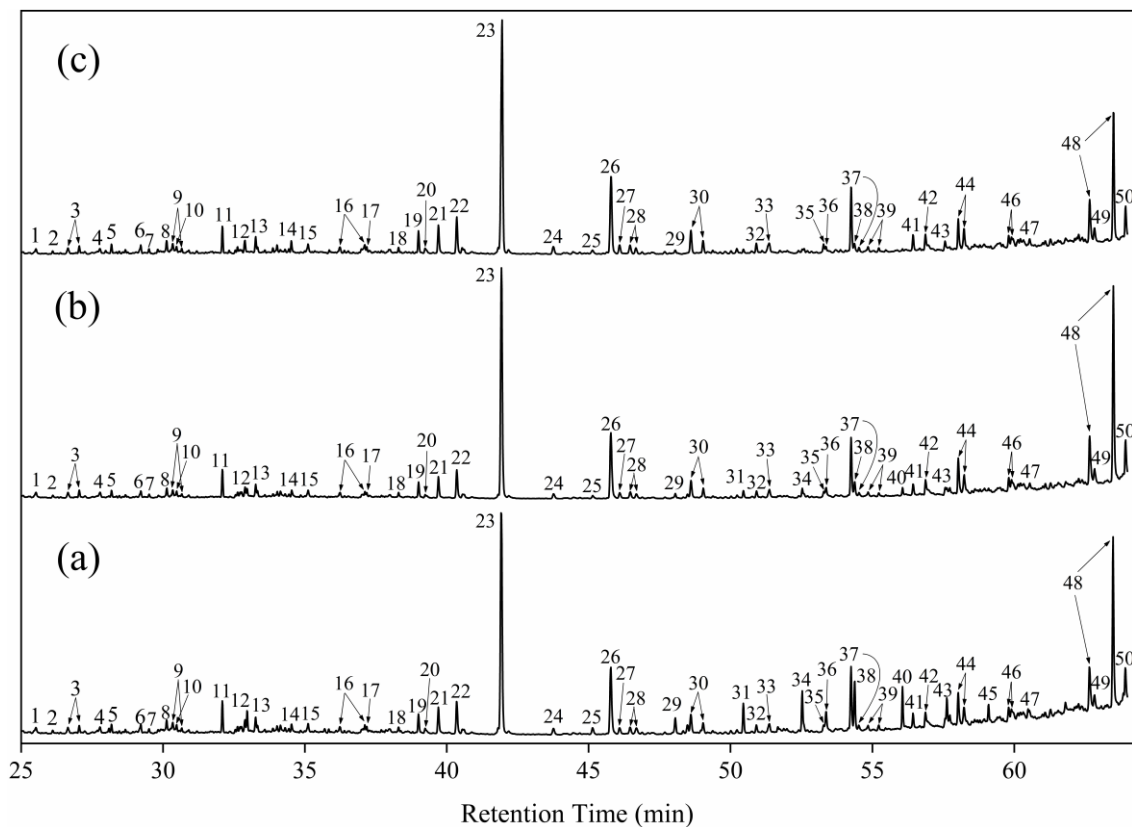
201 **Figure 3** Extraction yields for DCLR using liquefied DME, acetone, and hexane as the solvents.

202 almost complete; at this point, the mass ratio of DME/DCLR was approximately 70 and the extraction
 203 time was 40 min. Thus, approximately 40 min were required for complete extraction of 3g of DCLR at
 204 room temperature using 210 mL of liquefied DME as the solvent.

205 For an economical process, DME gas used for extraction must be recovered and recycled during the
206 practical application. Based on our previous studies [33], except for the DME dissolved in water, most of
207 the DME could be recovered. For example, when the feeding material was the coal with a moisture
208 content of up to 66.7 wt%, the recovery rate of DME was 95% [33]. Considering the moisture content of
209 the DCLR sample, which was quite low in this study, the recovery rate of DME could be ~100%.

210 Compared with DME extraction, Soxhlet methods were conducted at higher temperatures for a longer
211 extraction time of 6 h. The extraction yields using acetone and hexane as the solvents were 13.0% and
212 4.6%, respectively, which were lower than that using liquefied DME at 16.2% (**Figure 3**). **Table 2**
213 shows the performance of two extraction methods using liquefied DME and subcritical water as solvents.

214 The extraction yield using subcritical water as the solvent was defined on the dry basis of THF-
215 extractable fraction in the DCLR sample via Soxhlet extraction [18], which was different from that in
216 this study which defined the extraction yield on the dry ash-free basis of the DCLR sample. For
217 convenience and accuracy, the original extraction yields with different solvents were recalculated on the
218 dry basis of the DCLR sample and are listed in the column labeled 'Yield 2' in **Table 2**. Despite the
219 errors caused by the differences in used DCLR samples, the extraction yield (Yield 2) using liquefied
220 DME is 13.8 wt%, which is similar to the yield (Yield 2) obtained via subcritical water extraction at
221 320 °C and 11.7 MPa for 2 h with a low mass ratio of solvent/DCLR (14.4 wt%). Therefore, it can be
222 presumed that liquefied DME extraction method can be as effective as the subcritical water extraction
223 after optimization of factors such as extraction temperature, pressure, time, mass ratio of solvent/DCLR,
224 and the amount of water addition. This extraction method can be foreseen to have a stronger market
225 competitiveness owing to a shorter extraction time, lower energy consumption, and more convenient
226 separation of DME gas from the extract compared to conventional methods. Furthermore, the efficient
227 extraction of dry DCLR sample extends the application range of liquefied DME extraction technology,
228 as the previous studies regarding liquefied DME extraction mainly focused on wet feedstocks, such as



229

230 **Figure 4** GC-MS chromatogram of (a) DME-E, (b) Acetone-E, and (c) Hexane-E.

231 low-rank coal with high moisture contents, wet microalgae, and sludge.

232 3.2. Elemental composition of the extracts

233 **Table 1** shows the elemental compositions of the residues and extracts obtained using different solvents.

234 Each residue contains a slightly lower carbon content and a higher oxygen content relative to the

235 feedstock. However, hydrogen, nitrogen, and sulfur contents remain almost the same at 4%, 1%, and 2%,

236 respectively, which can account for the similar ratios of H/C and O/C in the feedstock and residues. The

237 elemental compositions of the extracts differ from the feedstock and residues, which include the highest

238 carbon and hydrogen contents of > 80% and 6%, respectively, highest ratio of H/C of 1.0, lowest ratio of

239 O/C of <0.1, and lowest content of sulfur of < 0.3%. These results are consistent with previous reports [2,

240 9]. Each extract had a VM content of > 90%, which was much higher than the feedstock (43%),

241 **Table 3** Light compounds determined using GC-MS in the extracts obtained from DCLR. ^a

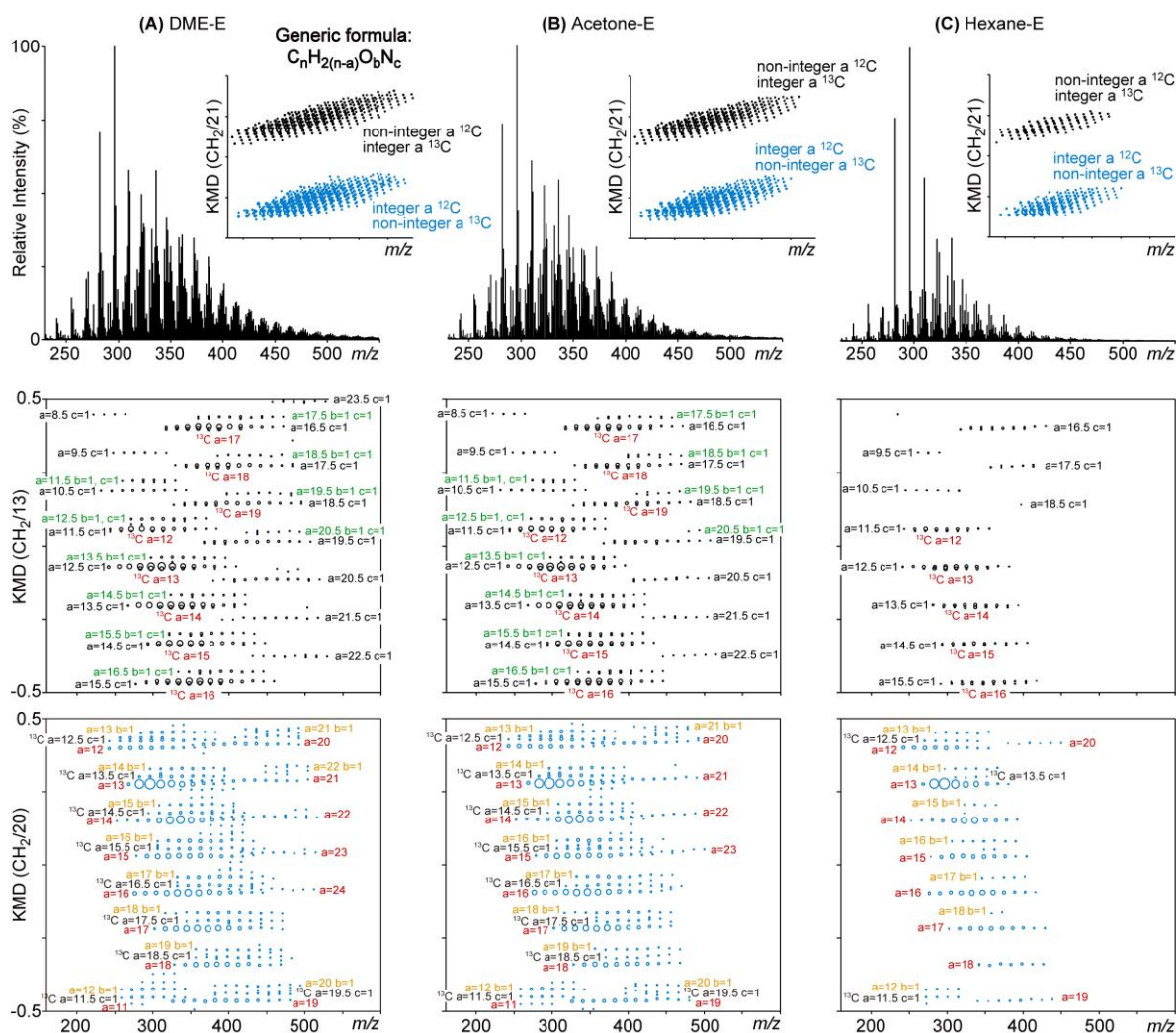
| No | Compound name | No | Compound name |
|----|---|----|--|
| 1 | 2,3,4,4a,9,9a-hexahydro-1H-fluorene | 26 | 1-methylpyrene |
| 2 | 6-propyl-1,2,3,4-tetrahydronaphthalene | 27 | 5,6-dihydro-4 <i>H</i> -benzo[<i>de</i>]anthracene |
| 3 | tetradecahydroanthracene | 28 | 4-methylpyrene |
| 4 | pentadecane | 29 | tricosane |
| 5 | 2-methyl-1,2-dihydronaphthalene | 30 | 1,3-dimethylpyrene |
| 6 | 6-butyl-1,2,3,4-tetrahydronaphthalene | 31 | Tetracosane |
| 7 | 1-ethoxynaphthalene | 32 | chrysen-6-ol |
| 8 | 1-(prop-1-en-2-yl)naphthalene | 33 | 2-methyl-7,12-dihydrotetraphene |
| 9 | 3-(<i>tert</i> -butyl)-1,2-dihydronaphthalene | 34 | pentacosane |
| 10 | hexadecane | 35 | 5-methoxybenzo[<i>c</i>]phenanthrene |
| 11 | hexadecahydroropyrene | 36 | isooctyl phthalate |
| 12 | 2,2'-dimethyl-1,1'-biphenyl | 37 | 8,9-dihydro-7 <i>H</i> -cyclopenta[<i>a</i>]pyrene |
| 13 | 1,2,3,4,5,6,7,8-octahydroanthracene | 38 | hexacosane |
| 14 | phenanthrene | 39 | 1,12-dimethyltetraphene |
| 15 | octadecane | 40 | heptacosane |
| 16 | 1,2,3,3a,4,5,9,10,10a,10b-decahydroropyrene | 41 | 7,12-dimethyltetraphene |
| 17 | nonadecane | 42 | benzo[<i>e</i>]acephenanthrylene |
| 18 | 4,5,9,10-tetrahydroropyrene | 43 | octacosane |
| 19 | 1,2,3,3a,4,5-hexahydroropyrene | 44 | benzo[<i>a</i>]pyrene |
| 20 | icosane | 45 | nonacosane |
| 21 | 1,2,3,6,7,8-hexahydroropyrene | 46 | 10-methylbenzo[<i>a</i>]pyrene |
| 22 | 4,5-dihydroropyrene | 47 | triacontane |
| 23 | pyrene | 48 | 1,12-benzoperylene |
| 24 | 2,3-Dihydro-1H-cyclopenta[<i>l</i>]phenanthrene | 49 | 1-phenylpyrene |
| 25 | docosane | 50 | anthanthrene |

242 ^a: Serial numbers corresponds to the numbers included in Figure 4.

243

244 accompanied with low contents of FC and ash. Overall, the elemental compositions of the residues or
 245 extracts obtained using different solvents were similar to each other. However, there was a subtle
 246 difference between extraction methods using hexane and the other two solvents. The nitrogen content in
 247 the feedstock was 1.0%, which was lower than those in DME-E and Acetone-E but higher than that in
 248 Hexane-E. Furthermore, the ash contents of DME-E and Acetone-E were as low as < 0.1%, whereas that
 249 of Hexane-E was 1.5%. Owing to high carbon contents, low sulfur and oxygen contents, and low ash
 250 contents of < 0.1%, DME-E and Acetone-E were determined to be naturally good feedstocks for high-
 251 grade carbon materials.

252 **3.3 Determination of light compounds**253 **Figure 4** displays the GC-MS chromatograms of DME-E, Acetone-E, and Hexane-E, and **Table 3**



254

255 **Figure 5** Mass and KMD analysis of (A) DME-E, (B) Acetone-E, and (C) Hexane-E. From top to
 256 bottom: LDI-HRMS spectrum and resolution-enhanced KMD plot (base unit: CH₂/21, threshold 1%);
 257 Filtered resolution-enhanced KMD plot from the monoisotopic C_nH_{2(n-a)}O_bN_c with non-integer a and ¹³C
 258 isotopes of C_nH_{2(n-a)}O_bN_c with integer a (black points, base unit: CH₂/13); Filtered resolution-enhanced
 259 KMD plot from the monoisotopic C_nH_{2(n-a)}O_bN_c with integer a and ¹³C isotopes of C_nH_{2(n-a)}O_bN_c with
 260 non-integer a (blue points, base unit: CH₂/20).

261 includes a list of light compounds identified by GC-MS. The compositions of the determined compounds
 262 in all three extracts are similar, including alkanes (C₁₄H₂₄~C₃₀H₆₂), cycloalkanes (such as

263 tetradecahydroanthracene and hexadecahydropyrene), and various monocyclic and polycyclic aromatic
264 compounds. The abundance of polycyclic aromatic hydrocarbons (PAHs) with two-, three-, four-, five-,
265 and six-membered benzene rings, which are represented by phenanthrene, pyrene, tetraphene,
266 benzo[*a*]pyrene, benzoperylene, anthanthrene, or their derivatives, supports that all the DCLR extracts
267 are potential materials that could be used to prepare high value-added carbon materials [15]. The
268 elemental composition of all the detected species can be conveniently denoted as $C_nH_{2(n-a)}O_b$ with
269 parameter *n* (C content) ranging from 11 to 30, parameter *a* (inverse of H content ~ degree of
270 unsaturation, $a=(2C-H)/2$) ranging from -1 for alkanes to 16 for highly unsaturated PAHs, and parameter
271 *b* (oxygen content) ranging from 0 to 4 in the fifty low molecular weight species detected by GC-MS
272 (**Figure 4**). This generic notation will be used in the next section for description of the carbonaceous
273 series with an identical unsaturation number and identical O content but a varying number of methylene
274 CH_2 moieties.

275 Compared to DME-E and Acetone-E, Hexane-E lacks some peaks of alkanes including tetracosane
276 ($C_{24}H_{50}$, No 31 in **Table 3**), pentacosane ($C_{25}H_{52}$, No 34 in **Table 3**), and heptacosane ($C_{27}H_{56}$, No 40 in
277 **Table 3**). However, the difference is small, and it can be concluded that liquefied DME, acetone, and
278 hexane can extract similar light compounds. To reveal the reason for a big difference in the extraction
279 yields of the three solvents, an additional characterization technique that allowed the detection of higher
280 molecular weight compounds was employed.

281 **3.4. Molecular composition**

282 In our previous studies, a simple LDI-HRMS mass analysis method combined with an appropriate
283 Kendrick mass defect analysis has been confirmed to be effective in characterizing the molecular
284 composition of coal or biomass extracts [32, 34]. The two LDI mass spectra recorded for DME-E and
285 Acetone-E are similar (**Figure 5 A-B**, top) while the third spectrum from Hexane-E appears different at
286 first sight (**Figure 5 C**, top). In the three spectra, the major ion series was assigned as $C_nH_{2(n-a)}$ with $a=13$
287 thanks to an accurate internal calibration (errors at ~1 ppm over the entire mass range). Nevertheless, a

288 thorough comparison of the chemical compositions requires the tedious assignment of the peaks one by
289 one in time-consuming processing.

290 Instead, a sequential KMD analysis dramatically facilitates the comparison using visual graphs and
291 speeds up the ability to make assignments via simulation of the theoretical KMDs (one KMD value per
292 series instead of one m/z value per ion) [32]. A first resolution-enhanced KMD plot was computed from
293 each of the full LDI mass spectra with $\text{CH}_2/21$ as the mathematical base unit (chemical moiety: CH_2 at
294 14.01565, divisor $X=21$). The plots instantly sorted the ~850-900 points that were generically labeled as
295 $\text{C}_n\text{H}_{2(n-a)}\text{O}_b\text{N}_c$ in two clouds by varying their contents of H (parameter a being integer or non-integer) and
296 ^{13}C isotopes (insets in **Figure 5** A-C, top). Each cloud that was composed of ~400-450 points was then
297 isolated and independently re-processed using $\text{CH}_2/13$ (**Figure 5** A-C, middle) and $\text{CH}_2/20$ (**Figure 5** A-
298 C, bottom) to further separate all the ion series depending on their O (parameter b), N (parameter c), and
299 unsaturation (parameter a, inverse of H content) contents. The resulting KMD plots display clear
300 horizontal alignments with one line per ions series with the elemental composition of the congeners
301 within a given series varying by $\pm n \cdot \text{CH}_2$ groups. There is no overlap because the resolution-enhanced
302 methodology takes advantage of the full spectral width of the plots from -0.5 to 0.5, which is in contrast
303 to the clustered KMD plots usually reported in the literature [35]. The Kendo spreadsheet now
304 incorporates a simulator which computes the theoretical KMD and mass-to-charge ratios (m/z) for a set
305 of parameters [36 ^{13}C , n] to instantly assign the ion series in the KMD plots. Several $\text{C}_n\text{H}_{2(n-a)}\text{O}_b\text{N}_c$
306 series are readily highlighted with $a=8.5-23.5$ (non-integer a, from lowest to highest degree of
307 unsaturation) / $a=12-24$ (integer a), $b=0-1$, and $c=0-1$ with their combination of $b=c=1$ and ^{13}C isotopes
308 in the two sets of plots for DME-E and Acetone-E (**Figure 5**, A-B, middle and bottom; red series: $b=c=0$,
309 $^{12}\text{C}/^{13}\text{C}$ isotopes; orange series: $b=1, c=0$; black series: $b=0, c=1, ^{12}\text{C}/^{13}\text{C}$ isotopes; green series: $b=c=1$).

310 The high similarity of their fully resolved KMD plots graphically confirms the high similarity of the
311 overall chemical composition of the two extracts in terms of high molecular weight species.

312 Considering its KMD plots, Hexane-E is also formed from similar classes of ion series that are generally
313 labelled $C_nH_{2(n-a)}O_bN_c$; however, the ranges of a, b, and c clearly differ with $a=9.5-18.5$ (non-integer a) /
314 $a=12-20$ (integer a), $b=0-1$, and $c=0-1$, while their combination is missing (**Figure 5**, C, middle and
315 bottom). Indeed, no singly oxygenated / nitrogenated series denoted as $C_nH_{2(n-a)}O_1N_1$ and labeled in
316 green in the previous KMD plots was detected for Hexane-E regardless of the mass range or the values
317 of n or a. The higher molecular weight compounds observable by LDI were clearly depleted in Hexane-
318 E in spite of being characterized under identical conditions of sample preparation and the parameters for
319 mass analysis. The potential of this last DCLR extracted with hexane is questionable due to a lower
320 amount and lower polycyclic character of the detected PAHs, as indicated by the narrower range for
321 parameter a, which revealed an overall lower degree of unsaturation. Thus, the extraction performed
322 with liquefied DME at room temperature, which was as good as the extraction with acetone at high
323 temperature considering their similar high molecular weight species, is preferred over extraction with
324 hexane at high temperature especially in terms of recovered PAHs.

325 **4. Conclusions**

326 The extraction of DCLR was performed at room temperature using liquefied DME. Approximately 40
327 min were required for the complete extraction of 3g of DCLR with 200-210 mL of liquefied DME. For
328 comparison, DCLR was extracted by the Soxhlet method using acetone and hexane; the extraction
329 temperature was above the boiling point of the solvent, and the extraction time was 6 h. Even so, the
330 extraction yield with liquefied DME was 16.2%, which was higher than the yields obtained from the
331 Soxhlet method with acetone and hexane, at 13.0% and 4.6%, respectively. Furthermore, the energy
332 consumption during the DME extraction process was low because the extraction was performed at room
333 temperature and DME gas separated from the extract without heating. DME-E and Acetone-E contain
334 high carbon contents, low sulfur and oxygen contents, and low ash contents of $< 0.1\%$; thus, they can be
335 used as feedstocks of carbon materials. The GC-MS results showed that the extracts obtained using the
336 three different solvents had similar light compound compositions and are abundant in PAHs with two-,

337 three-, four-, five-, and six-membered benzene rings, represented by phenanthrene, pyrene, tetraphene,
338 benzo[*a*]pyrene, benzoperylene, anthanthrene, and their derivatives. The molecular compositions of the
339 extracts were investigated by a simple LDI-HRMS mass analysis combined with an appropriate
340 Kendrick mass defect analysis. It revealed that the extraction performed with liquefied DME at room
341 temperature was equally effective as the extraction with acetone at high temperature considering their
342 compositional similarity in high molecular weight species and should be preferred over extraction with
343 hexane at high temperature, particularly considering the recovered PAHs. All results above confirm that
344 liquefied DME is an efficient and economic solvent for extracting DCLR.

345

346 **Abbreviations**

347 DME dimethyl ether

348 DCL direct coal liquefaction

349 ICL indirect coal liquefaction

350 DCLR direct coal liquefaction residue

351 PASs polycyclic aromatic structures

352 PAHs polycyclic aromatic hydrocarbons

353 HPLC high-performance liquid chromatography

354 THF tetrahydrofuran

355 VM volatile matter

356 FC fixed carbon

357 GC/MS gas chromatograph/mass spectrometer

358 LDI-HRMS laser desorption ionization high-resolution mass spectra

359 NaTFA sodium trifluoroacetate

360 KMD Kendrick mass defect

361 VBA Visual Basic for application coding

362

363 **Acknowledgements**

364 This work was supported by JSPS KAKENHI Grant Numbers JP23686117 (H. Kanda).

365

366 **Competing Interests**

367 There are no competing interests.

368

369 **References:**

370 [1] Vasireddy S, Morreale B, Cugini A, Song Cs, Spivey JJ. Clean liquid fuels from direct coal
371 liquefaction: Chemistry, catalysis, technological status and challenges. *Energy & Environmental Science*
372 2011;4:311-45.

373 [2] Lin XC, Li SY, Guo FH, Jiang GC, Chen XJ, Wang YG. High-efficiency extraction and
374 modification on the coal liquefaction residue using supercritical fluid with different types of solvents. *Energy*
375 *& Fuels* 2016;30:3917-28.

376 [3] Li Y, Zhang XP, Dong HF, Wang XL, Nie Y, Zhang SJ. Efficient extraction of direct coal
377 liquefaction residue with the bmim cl/nmp mixed solvent. *RSC Advances* 2011;1:1579-84.

378 [4] Cui H, Yang JL, Liu ZY, Bi JC. Characteristics of residues from thermal and catalytic coal
379 hydroliquefaction. *Fuel* 2003;82:1549-56.

380 [5] Khare S, Dell'Amico M. An overview of conversion of residues from coal liquefaction processes.
381 *Canadian Journal of Chemical Engineering* 2013;91:1660-70.

382 [6] Yang JL, Wang ZX, Liu ZY, Zhang YZ. Novel use of residue from direct coal liquefaction process.
383 *Energy & Fuels* 2009;23:4717-22.

384 [7] Wang C, Xu SP, Wang GY, Xiao YH. Pyrolysis of coal hydroliquefaction residue in a dual loop
385 reaction system. *Fuel* 2018;212:448-54.

- 386 [8] Li J, Yang JL, Liu ZY. Hydro-treatment of a direct coal liquefaction residue and its components.
387 *Catalysis Today* 2008;130:389-94.
- 388 [9] Wang YG, Niu ZS, Shen J, Bai L, Niu YX, Wei XY, et al. Extraction of direct coal liquefaction
389 residue using dipropylamine as a CO₂-triggered switchable solvent. *Fuel Processing Technology* 2017;159:27-
390 30.
- 391 [10] Zhou Y, Xiao N, Qiu JS, Sun YF, Sun TJ, Zhao ZB, et al. Preparation of carbon microfibers from
392 coal liquefaction residue. *Fuel* 2008;87:3474-6.
- 393 [11] Xiao N, Zhou Y, Qiu JS, Wang ZH. Preparation of carbon nanofibers/carbon foam monolithic
394 composite from coal liquefaction residue. *Fuel* 2010;89:1169-71.
- 395 [12] Zhang JB, Jin LJ, Zhu SW, Hu HQ. Preparation of mesoporous activated carbons from coal
396 liquefaction residue for methane decomposition. *Journal of Natural Gas Chemistry* 2012;21:759-66.
- 397 [13] Zhang JB, Jin LJ, Cheng J, Hu HQ. Hierarchical porous carbons prepared from direct coal
398 liquefaction residue and coal for supercapacitor electrodes. *Carbon* 2013;55:221-32.
- 399 [14] Li P, Zhao YQ, Fan GX. Quantitative analysis of alkanolate and condensed arenes in the extracts
400 from direct coal liquefaction residue by ultrasonication-assisted solvent extraction using alcohols. *Energy*
401 *Sources, Part A: Recovery, Utilization, and Environmental Effects* 2018;40:1266-72.
- 402 [15] Wang YG, Niu ZS, Shen J, Niu YX, Liu G, Sheng QT. Optimization of direct coal liquefaction
403 residue extraction. *Energy Sources Part a-Recovery Utilization and Environmental Effects* 2017;39:83-9.
- 404 [16] Liu PF, Zhang YQ, Fang YT, Zhao JT. Supercritical solvent extraction of direct liquefaction residue
405 from shenhua coal. *J Fuel Chem Technol* 2012;40:776-81.
- 406 [17] Jiang GC, Lin XC, Zhang SJ, Wang ZQ, Wang YG, Chen Q, et al. Supercritical fluid extraction of
407 direct coal liquefaction residue basing on hansen solubility parameters. *Chemical Journal of Chinese*
408 *Universities-Chinese* 2015;36:544-50.
- 409 [18] Jiang XJ, Cui H, Liu MX, Guo Q, Xu J, Yang JL, et al. Extracting coal liquids from direct coal
410 liquefaction residue using subcritical water. *Energy & Fuels* 2016;30:4520-8.

- 411 [19] Nie Y, Bai L, Li Y, Dong HF, Zhang XP, Zhang SJ. Study on extraction asphaltenes from direct coal
412 liquefaction residue with ionic liquids. *Industrial & Engineering Chemistry Research* 2011;50:10278-82.
- 413 [20] Li Y, Zhang XP, Lai SY, Dong HF, Chen XL, Wang XL, et al. Ionic liquids to extract valuable
414 components from direct coal liquefaction residues. *Fuel* 2012;94:617-9.
- 415 [21] Nie Y, Bai L, Dong HF, Zhang XP, Zhang SJ. Extraction of asphaltenes from direct coal liquefaction
416 residue by dialkylphosphate ionic liquids. *Separation Science and Technology* 2012;47:386-91.
- 417 [22] Wang JL, Yao HW, Nie Y, Bai L, Zhang XP, Li JW. Application of iron-containing magnetic ionic
418 liquids in extraction process of coal direct liquefaction residues. *Industrial & Engineering Chemistry
419 Research* 2012;51:3776-82.
- 420 [23] Bai L, Nie Y, Huang JC, Li Y, Dong HF, Zhang XP. Efficiently trapping asphaltene-type materials
421 from direct coal liquefaction residue using alkylsulfate-based ionic liquids. *Fuel* 2013;112:289-94.
- 422 [24] Bai L, Nie Y, Li Y, Dong HF, Zhang XP. Protic ionic liquids extract asphaltenes from direct coal
423 liquefaction residue at room temperature. *Fuel Processing Technology* 2013;108:94-100.
- 424 [25] Holldorff H, Knapp H. Binary vapor-liquid-liquid equilibrium of dimethyl ether-water and mutual
425 solubilities of methyl chloride and water: Experimental results and data reduction. *Fluid Phase Equilibria*
426 1988;44:195-209.
- 427 [26] Catchpole OJ, Tallon SJ, Grey JB, Fletcher K, Fletcher AJ. Extraction of lipids from a specialist
428 dairy stream. *J Supercrit Fluid* 2008;45:314-21.
- 429 [27] Authority EFS. Safety in use of dimethyl ether as an extraction solvent. *EFSA Journal* 2009;7:984.
- 430 [28] Catchpole O, Moreno T, Montañes F, Tallon S. Perspectives on processing of high value lipids using
431 supercritical fluids. *The Journal of Supercritical Fluids* 2018;134:260-8.
- 432 [29] Office TS. Japanese pharmacopoeia-seventeenth edition. 2016.
- 433 [30] Strohalm M, Kavan D, Novák P, Volný M, Havlíček V. Mmass 3: A cross-platform software
434 environment for precise analysis of mass spectrometric data. *Analytical Chemistry* 2010;82:4648-51.
- 435 [31] Nakamura S, Cody RB, Sato H, Fouquet T. Graphical ranking of divisors to get the most out of a
436 resolution-enhanced kendrick mass defect plot. *Analytical Chemistry* 2019;91:2004-12.

- 437 [32] Zheng QX, Morimoto M, Sato H, Fouquet T. Resolution-enhanced kendrick mass defect plots for the
438 data processing of mass spectra from wood and coal hydrothermal extracts. *Fuel* 2019;235:944-53.
- 439 [33] Kanda H, Makino H, Miyahara M. Energy-saving drying technology for porous media using
440 liquefied dme gas. *Adsorption-Journal of the International Adsorption Society* 2008;14:467-73.
- 441 [34] Zheng Q, Morimoto M, Sato H, Takanohashi T. Molecular composition of extracts obtained by
442 hydrothermal extraction of brown coal. *Fuel* 2015;159:751-8.
- 443 [35] Fouquet T, Sato H. Extension of the kendrick mass defect analysis of homopolymers to low
444 resolution and high mass range mass spectra using fractional base units. *Analytical Chemistry* 2017;89:2682-6.
- 445 [36] Constant pressure liquefied petroleum gas extraction tool for micro gas turbine, has flexible resin
446 water jacket covering the gas cylinder, in which warm water flow path is formed. Iwatani Ind Co Ltd.
- 447

Figure 1

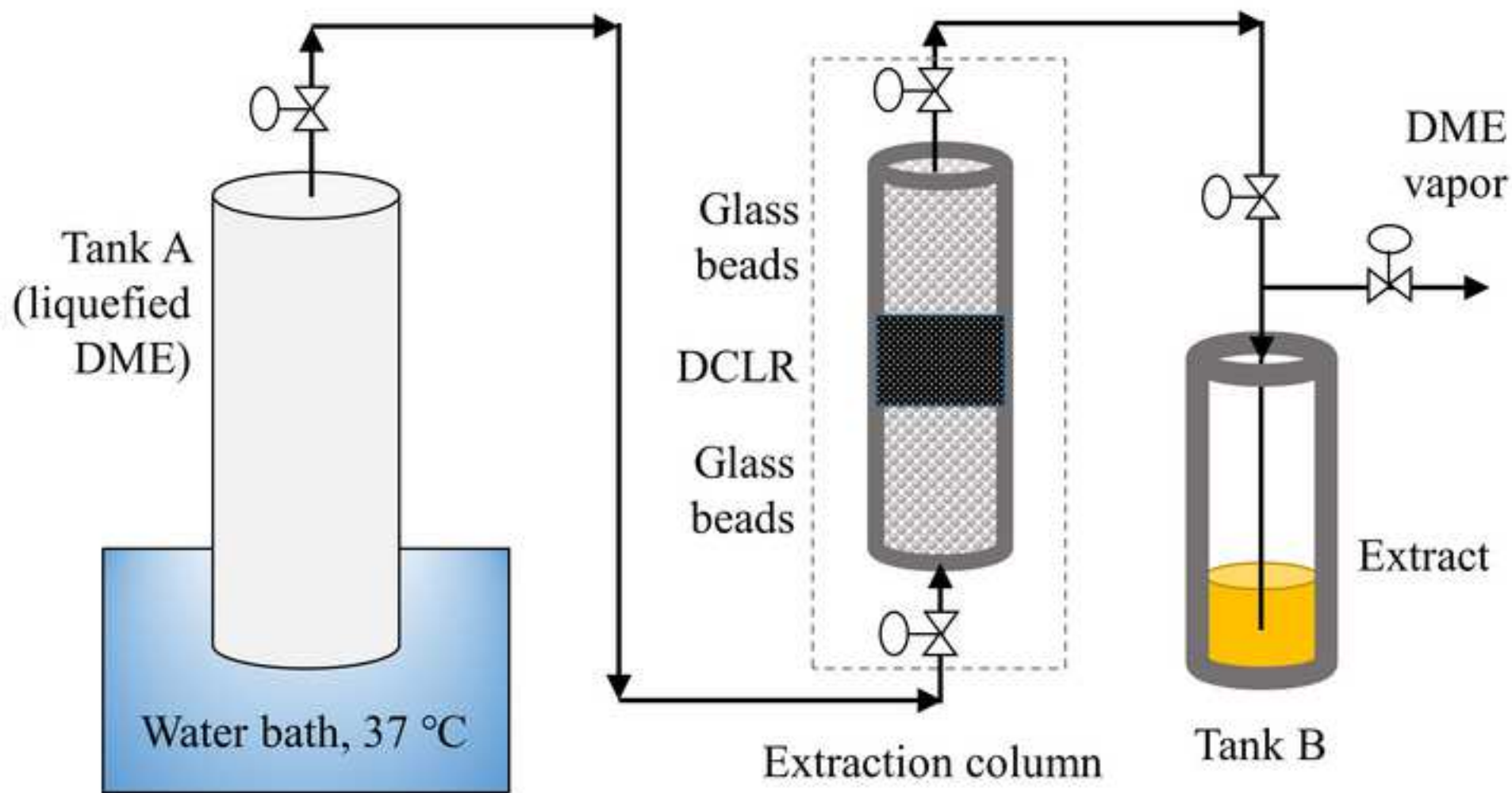


Figure 2

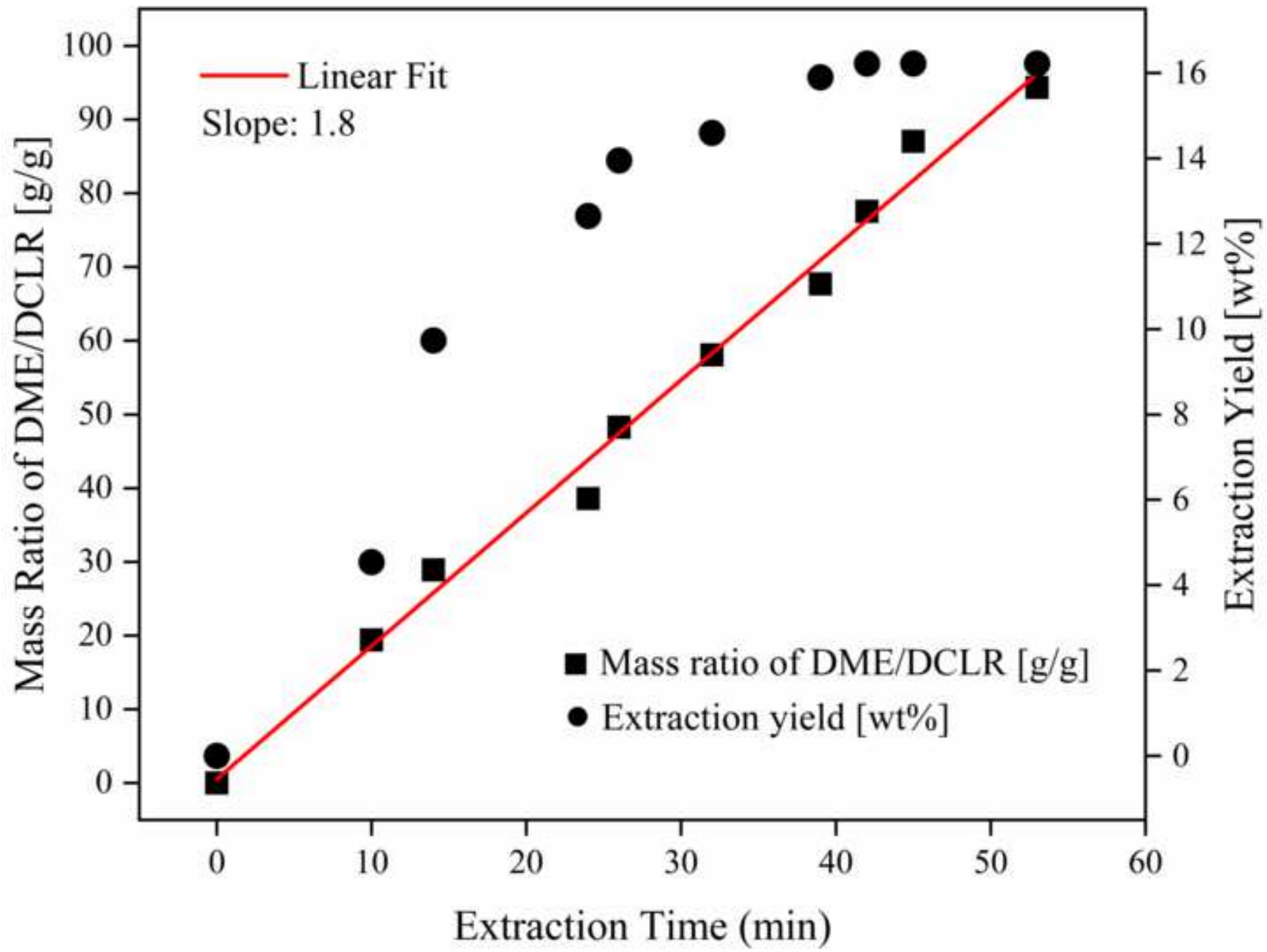


Figure 3

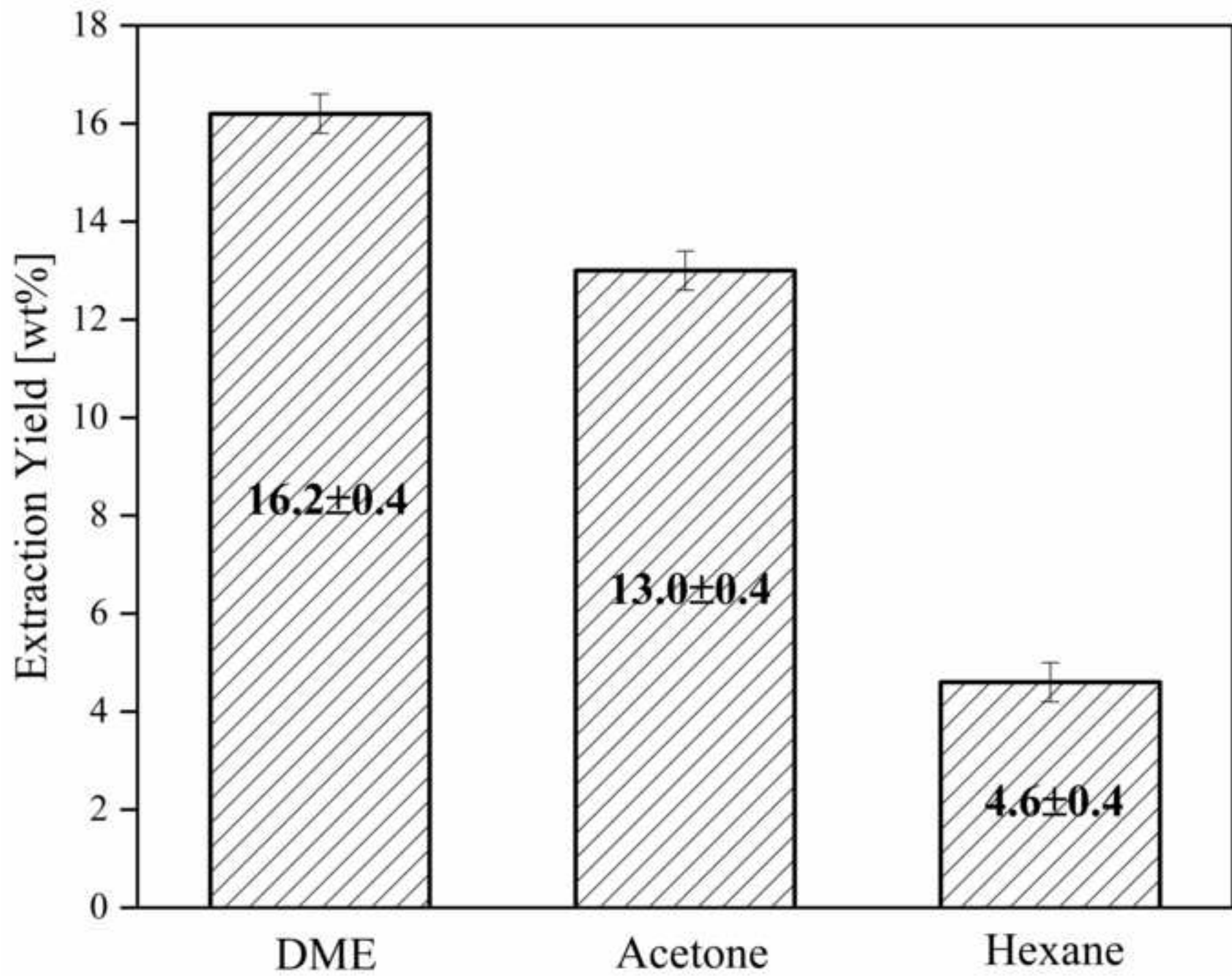


Figure 4

